SYNTHETIC THERMAL IMAGE GENERATION USING HEAT TRANSFER MODELING

RUDI HERIANSYAH[1], U. U. SHEIKH[2], & S. A. R. ABU-BAKAR[3]

Abstract. Thermal image is an image that shows the thermal or temperature properties of an object. Thermal image of an object is obtained from a thermal infrared camera. This camera works by employing radiative heat transfer principles and uses sensors to capture the radiated energy of an object. Thermal image of an object in the real world which is captured by a thermal camera is a real thermal image of that object. But sometimes there is a situation in which it is necessary to simulate a real situation in order to generate synthetic thermal image, for example in estimating the temperature distribution or in understanding the thermal behaviour of a particular object. This paper demonstrates the technique to generate the synthetic thermal images, all which is based on image processing paradigm.

Keywords: Synthetic thermal image; numerical heat transfer; infrared thermography

Abstrak. Imej haba adalah imej yang menunjukkan ciri haba atau suhu daripada sebuah objek. Imej haba ini diperolehi dengan menggunakan kamera haba inframerah. Kamera ini bekerja menggunakan prinsip radiasi perpindahan haba dan menggunakan penderia untuk membaca radiasi tenaga sebuah objek. Imej haba dari sesuatu objek di dunia nyata adalah imej haba sebenar dari objek berkenaan. Walau bagaimanapun ada situasi tertentu yang mana imej haba tiruan diperlukan, misalnya untuk mengira pengagihan suhu atau untuk memahami perilaku haba sebuah objek. Kertas kerja ini memperlihatkan cara untuk mendapatkan imej haba tiruan ini, yang berdasarkan pada paradigma pemprosesan imej.

Kata kunci: Imej haba tiruan; perpindahan haba berangka; termografi inframerah

1.0 INTRODUCTION

Thermal image is an image that shows thermal or temperature properties of an object. The term *thermal* refers to heat or hot energy and usually, this is called as *hot-spot*. A hot-spot in an object can reflect an abnormal situation or condition occurring in that object. The hot-spot can be a sign to an internal fault, hidden defective region, abnormal operation or anything that indicates that something is wrong.

Thermal image of an object is obtained from a thermal infrared camera. This camera works by employing radiative heat transfer principles and uses sensors to

[1] Faculty of Engineering, Multimedia University, Cyberjaya Campus, 63100 Cyberjaya, Selangor
Tel: 03-83125164. Email: rudihe@gmail.com
[2&3] Computer Vision, Video & Image Processing Lab. (CVVIP), Fac. of Electrical Engineering, Universiti Teknologi Malaysia, 81310 UTM Skudai, Johor Bahru, Malaysia
Tel: 07-5535274; Fax: 07-5566272. Email: syed@fke.utm.my

capture the radiated energy of an object [1]. This kind of technology is called as infrared thermography (IRT) [2], and it is one of many techniques in nondestructive testing (NDT) [3]. As implied by its name, IRT uses the distribution (suffix *–graphy*) of surface temperature (prefix *thermo-*) to assess the structure or behaviour of what is under the surface [4].

The thermal image of an object in the real world which is captured by a thermal camera is the real thermal image of that object. But sometimes there is a situation in which it is necessary to simulate a real situation in order to generate synthetic thermal image, for example to estimate the temperature distribution or to understand the thermal behaviour of an object, so that with a controlled environment and with known parameters, the result can be properly predicted.

Nowakowski *et al.* [5] uses synthetic thermal pictures to improve diagnostics in medicine. The specific time constant synthetic images were generated by the principle of pulsed thermography. They defined some parameters that relate the temperature values to the time constants. Weijie *et al.* [6] used the principles of heat transfer based on two dimensional implicit finite difference technique to calculate the surface temperature of an object and to generate infrared image of the object. Gambotto [7] combined the synthetic thermal image with the real image to generate realistic infrared images of outdoor scenes. The generation method is similar as in [6] by using the principles of heat transfer. Evans [8] modeled the thermal warming and cooling of an object to simulate forward looking infrared (FLIR) imagery using electrical circuit principles of the heat transfer. Oh *et al.* [9] modeled accurate IR images of an object by using octree. However, these works take no account of non-homogeneous structured material and the internal heat source of the object.

This paper uses the finite element based numerical heat conduction method to generate the synthetic image of a high temperature object such as an industrial furnace wall. Finite element method (FEM) has some advantages over finite difference method (FDM) in the context of its generalization and its proper application to deformed object models [10]. The synthetic thermal images are generated to simulate the defective wall of a furnace and its temperature distribution on the other surface of the non-defective wall. The first step is to build the model, and then to simulate the numerical heat conduction. Lastly based on the temperature values, a synthetic thermal image of the non-defective wall is generated. The generation mechanism based on this method is described in this paper.

2.0 MODEL DESCRIPTION

The model for this study is taken from [11] but with the addition of a steel wall as the outer surface (cold-face) wall as shown in Figure 1. The model is selected because it represents the actual situation of refractory layered wall [23]. A multiple layer wall of a furnace consists of a firebrick layer (22 cm), an insulation wall (11 cm), a ceramic
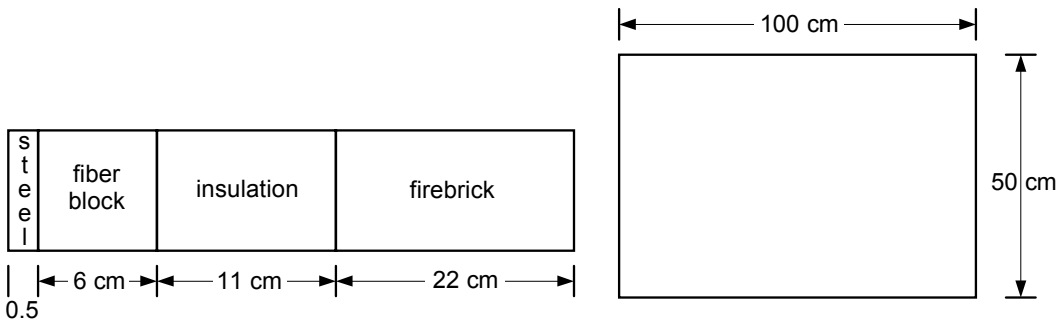
Figure 1   Typical four layer furnace wall and its front-side view

fiber block (6 cm) and an AISI 316 stainless steel (0.5 cm). For studying purposes, we will concentrate our analysis on an area of 1 m × 0.5 m.

2.1   Simulated Defect Model

This paper will generate the synthetic thermal image of a defective wall, and the defect type to be modeled is the spalling defect. Spalling defect is defined as "the breaking or cracking of refractory brick in service, to such an extent that pieces are separated or felt away, leaving new surfaces of the brick exposed." Spalling of refractory brick is of three general types: thermal spalling, mechanical spalling, and structural spalling [12]. The model was designed with SolidWorks [13], and the defect was embedded within the hot-face refractory wall (22 cm wall). Size of defect was fixed to 15 cm^2 with depth of 15 cm from the hot-face wall (Figure 2).
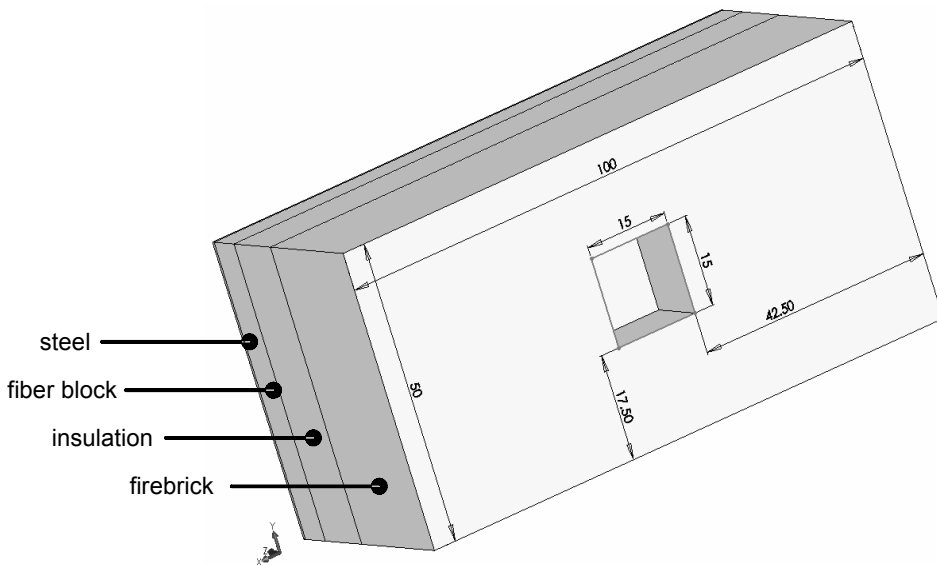

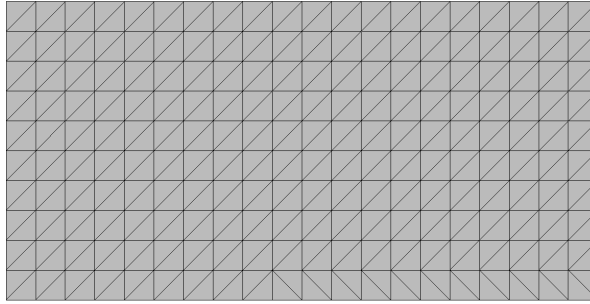**Figure 2**   Refractory wall with spalling defect with 34.5 cm depth

Figure 3   View of cold-face wall of the model after meshing

3.0   SIMULATION RESULT

The simulations for this study involved three dimensional finite element models. COSMOSWorks [14] was employed for the thermal study and the model was meshed with the coarse element size of 5 cm and the tolerance approximate to 0, hence there will be 11×21 nodes in row and column direction respectively. Figure 3 shows the view of the cold-face wall after meshing. The nodal temperature values on this wall which will be then used to generate a synthetic thermal image.

In this simulation, it is assumed that the temperature has been at its steady-state condition, hence hot-face wall temperature was constant at 1100°C, while ambient temperature assumed to be at 25°C. Adiabatic boundary conditions are applied to the four sides of the wall, thus there are no losses through these sides as they are assumed to be insulated. Losses due to convective (h = 10 W/m^2.K) and radiative (ε = 0.5) heat transfer occurred from the outer surface (cold-face) wall. Thermal properties of the model are given in Table 1. Temperature distribution result within the wall for a certain spalling size and depth is shown in Figure 4. In the figure, the red colour represents higher temperature section and the blue colour represents lower temperature section. It is obvious from the figure that the hot temperature at the inside surface wall gradually decreases to the outer surface wall. Another fact is that the temperature at the outside wall (at the position where the defect is located in

Table 1   Thermal properties of the model

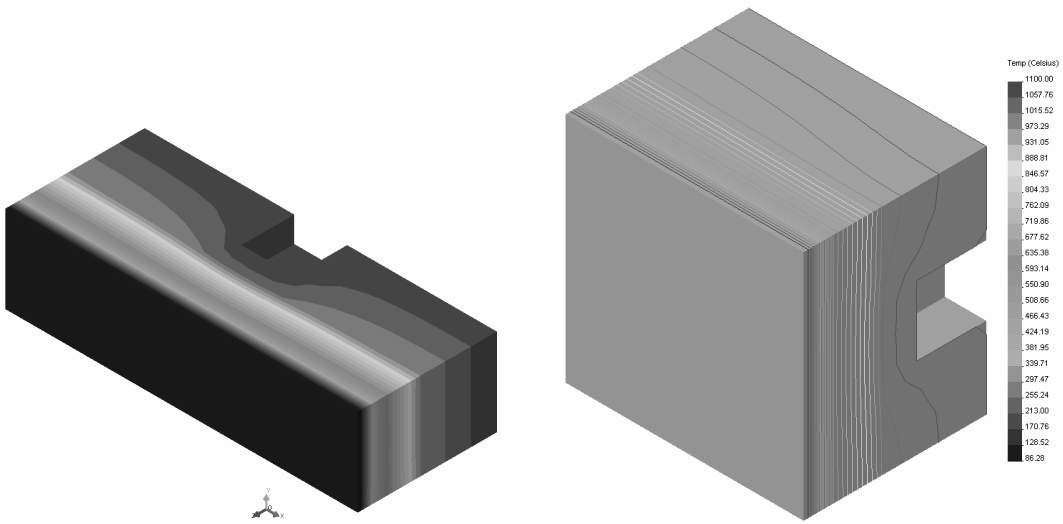| Wall Type	Thermal Conductivity (W/m.K)	Specific Heat (J/kg.K)	Density (kg/m^3)
Firebrick	1.436	0.96	2300
Insulation	0.225	1.3	1200
Ceramic fiber block	0.116	2.8	430
AISI 316 Stainless steel	16.3	499.99	8000

Figure 4   Middle-bottom half-section view (left), right-middle half-section view of temperature distribution within the walls (right) (size = 15 cm^2, depth = 15 cm)

the inside surface wall) is hotter than surroundings due to the shorter length of the layered walls.

4.0   SYNTHETIC THERMAL IMAGE GENERATION

Simulation from the previous section provides the temperature nodal values data of size 11×21 or 231 nodes, which are in Celsius degree. The synthetic thermal image will be generated based on these temperature values. The process flow for synthetic thermal image generation is as shown in the Figure 5. The discussion for this process is described in the following section.
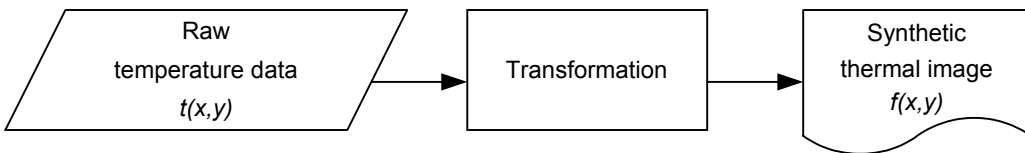

Figure 5   Synthetic thermal image generation process

4.1   Image Representation

A digital image may be defined as a two-dimensional function, $f(x,y)$, where x and y are *spatial* (plane) *coordinates*, and the amplitude of f at any pair of coordinates (x,y)

is called the intensity of the image at that point [16]. In a digital computer, it is required to represent images as two-dimensional arrays of points. A point on the 2-D grid is called a *pixel* or *pel*. Both words are abbreviations of the word picture element.

In the simplest case, the pixels are located on a rectangular grid. The position of the pixel is given in the common notation for matrices. The first index, m, denotes the position of the row, the second, n, the position of the column (Figure 6). If the digital image contains $M \times N$ pixels, *i. e.*, is represented by an $M \times N$ matrix, the index n runs from 0 to N–1, and the index m from 0 to M–1. M gives the number of rows, N the number of columns [17].

A digital thermal image (or shortly thermal image) has similar notation with a digital image (or shortly an image). *Thermogram* is a common name for a thermal image and the common term for a digital image is a *visual* image. In a thermogram, $f(x,y)$, defined as a 2-D radiance function and the value of f at any point (x,y) is proportional to the radiance or energy emitted from the scene at that location.

The raw radiometric data obtained from an infrared camera is generally either of 8, 12, 14, or 16 bits, giving $2^8 = 256$ (0 to 255), $2^{12} = 4096$ (0 to 4095), $2^{14} = 16,384$ (0 to 16383), or $2^{16} = 65,536$ (0 to 65,355) intensity values. In this paper, 8 bit gray-level is applied when generating the synthetic thermal image.
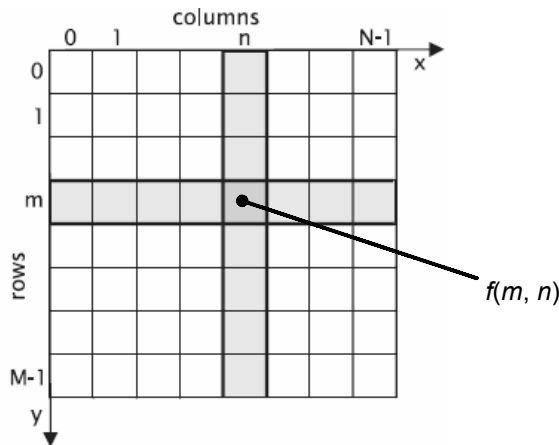

Figure 6   Image representation

The following section discusses on the technique in generating this thermogram based on its raw temperature data. There are two schemes for this purpose: first, *grayscale* thermogram and second, *color* thermogram using *RGB* colour space. In color image terminology, the latter coloring mechanism commonly known as *pseudo-* or *false-color* image.

4.2   Grayscale Thermogram

In infrared thermography, usually low intensities in a thermogram are represented with dark shades and high intensities with bright shades [4], but this is not always the case, since the vice versa scheme can also be applied. For this two color modes: it is called as *Black* → *White* (B → W) color map if the dark shades represent low intensities or low temperature value, or *White* → *Black* (W → B) color map if the bright shades represent low intensities or low temperature value.
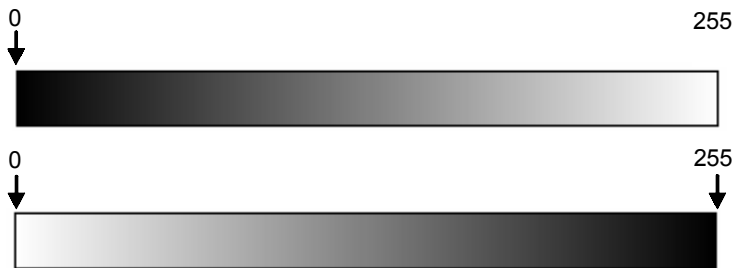

Figure 7   (B → W) and (W → B) color bar

For 8 bit color system, low intensities (low temperature values) are represented by 0 and high intensities represented by 255 in the case of (B → W) color map, and vice versa for the case of (W → B) color map. Color bar illustration (using full intensity values) for these two cases is shown in Figure 7.

The transformation or mapping process from radiometric raw data (temperature values) to intensities values can be done straightforward. Let T and I denotes the temperature values and intensity value respectively. $T_{k=1}^{K}$ is the temperature value from $k = 1$ to K. $I_{i_{min}}^{i_{max}}$ is the gray-level value that will be used for mapping process, from i_{min} to i_{max} and as mentioned previously, we just concentrate on 8 bit system, hence the maximum value for i_{max} is always equal to 255. For simplicity, the discussion in this paper is limited to $K \leq 256$.

The first step is to sort the raw data in *ascending* order to generate (B → W) color map or in *descending* order for (W → B) mapping. Then, calculate numbers of temperature value level K. After that, determine starting gray-level value i_{min} that will be employed, and assign all values to gray-level values. For (B → W) case $T_1 = i_{min}$, $T_2 = i_{min} + 1$, ..., $T_K = I_{K + i_{min}}$ (Figure 8) or $T_K = i_{min}$, $T_{K-1} = i_{min} + 1$, ..., $T_1 = I_{K + i_{min}}$ for (W → B) mapping. This mapping process is just applied to one column vector (one color plane), therefore when generating actual image in any format, another two color planes are assigned to this mapped color plane. Since equal intensities of each *red*, *green* and *blue* color channel will display that image as a greyscale image.
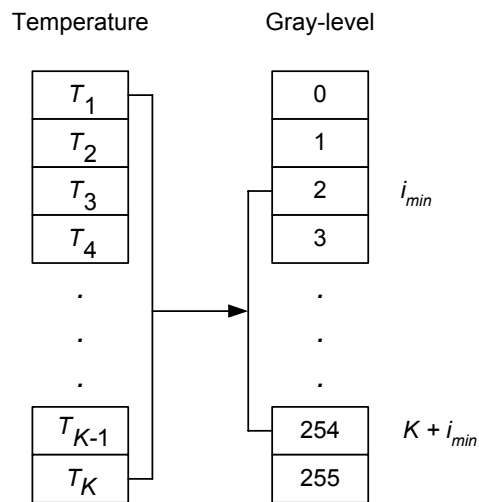
Figure 8   Mapping from temperature to intensity value

Figure 9   Synthetic greyscale thermogram: B → W (top), W → B (bottom)

Figure 9 shows the generated synthetic thermal image in grayscale format, both for (B → W) and (W → B) respectively. It is obvious from the figure that low temperature value will have low intensity value and high temperature has high intensity (as shown in the centre of the image) for (B → W) mapping, and vice versa situation is occurred in (W → B) mapping. Note that thermograms in the figure are scaled for displaying purpose only. Readers who are interested on the image scaling mechanism can refer to the standard literature [21].

4.3   Color Thermogram

The use of color in image processing is motivated by two principal factors. First, color is a powerful descriptor that often simplifies object identification and extraction from a scene. Second, humans can discern thousands of color shades and intensities, compared to about only two dozen shades of gray [18].

Color image processing is divided into two major areas: *full-color* and *pseudo-color* processing. In the first category, the images in question typically are acquired with a full-color sensor, such as a color TV or color scanner. In the second category, the problem is one of assigning a color to a particular monochrome intensity or range of intensities. Until recently, most digital color image processing was done at the pseudo-color level.

4.3.1 Thermogram Generation

The procedure to generate a color thermogram is similar to the generation of grayscale thermogram described in the previous section. But in generating color thermogram, the each temperature values are mapped to the three RGB components. These RGB values are usually known as *color scale* or *color ramp* [19]. The most commonly used color scale is often refered to as *hot-to-cold* or *blue-to-red* (B → R) color scale. Blue is chosen for the low values, green for middle values, and red for the high bounds. Cyan and yellow are added so that the color scales only move along the edges of the color cube [20]. The path of this color scheme within color cube is shown in Figure 10.

Color transition for (B → R) color scale is shown in the Figure 11. This color is generated using the standard color table as shown in Table 2 [20]. It is easy to understand that the color runs from blue, cyan, green, yellow, and red.

For color synthetic thermal image generation, each temperature value is mapped to its RGB value after sorting the data in ascending order, meaning that *blue* represents low temperature and *red* represents hot temperature. Color thermogram version for the temperature data using (B → R) color scale is shown in Figure 12. This synthetic thermal image is easier to interpret and gives more intuitive sense for fast decision making to a thermographer.
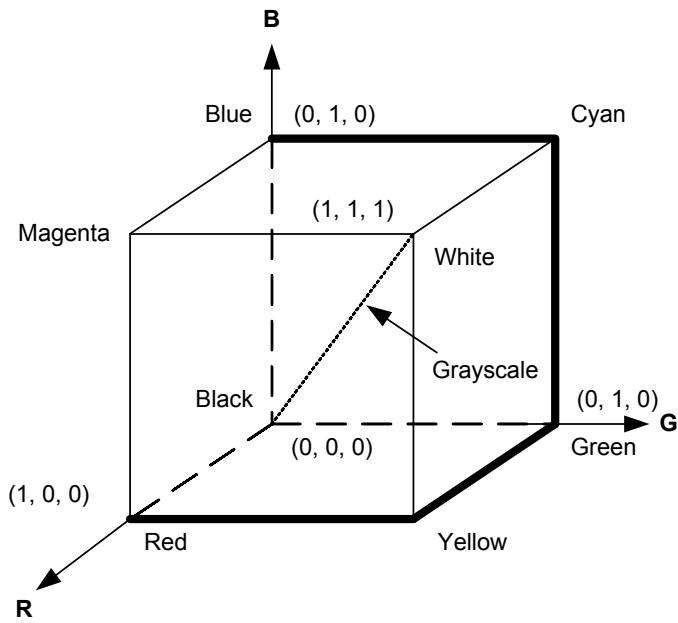
Figure 10   (B ➔ R) color scale within color cube

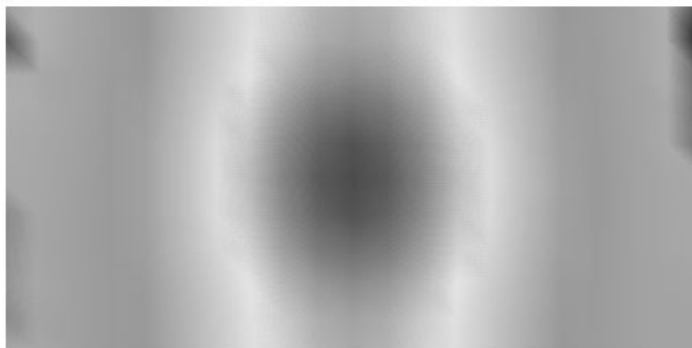**Figure 11**   (B ➔ R) color transition

Figure 12   Color thermogram of temperature data

Table 2   A standard (B ➔ R) color scale

ID	R	G	B	ID	R	G	B	ID	R	G	B	ID	R	G	B
0	0	0	255	65	0	255	249	130	9	255	0	195	255	239	0
1	0	3	255	66	0	255	246	131	13	255	0	196	255	236	0
2	0	7	255	67	0	255	241	132	17	255	0	197	255	231	0
3	0	11	255	68	0	255	238	133	21	255	0	198	255	228	0
4	0	15	255	69	0	255	233	134	25	255	0	199	255	223	0
5	0	19	255	70	0	255	230	135	29	255	0	200	255	220	0
6	0	23	255	71	0	255	225	136	33	255	0	201	255	215	0
7	0	27	255	72	0	255	222	137	37	255	0	202	255	212	0
8	0	31	255	73	0	255	217	138	41	255	0	203	255	207	0
9	0	35	255	74	0	255	214	139	45	255	0	204	255	204	0
10	0	39	255	75	0	255	209	140	49	255	0	205	255	199	0
11	0	43	255	76	0	255	206	141	53	255	0	206	255	196	0
12	0	47	255	77	0	255	201	142	57	255	0	207	255	191	0
13	0	51	255	78	0	255	198	143	61	255	0	208	255	188	0
14	0	55	255	79	0	255	193	144	66	255	0	209	255	183	0
15	0	59	255	80	0	255	190	145	70	255	0	210	255	180	0
16	0	63	255	81	0	255	185	146	74	255	0	211	255	175	0
17	0	67	255	82	0	255	182	147	78	255	0	212	255	172	0
18	0	71	255	83	0	255	177	148	82	255	0	213	255	167	0
19	0	75	255	84	0	255	174	149	86	255	0	214	255	167	0
20	0	79	255	85	0	255	169	150	90	255	0	215	255	159	0
21	0	83	255	86	0	255	166	151	94	255	0	216	255	156	0
22	0	87	255	87	0	255	161	152	98	255	0	217	255	151	0
23	0	91	255	88	0	255	158	153	102	255	0	218	255	148	0
24	0	95	255	89	0	255	153	154	106	255	0	219	255	143	0
25	0	99	255	90	0	255	150	155	110	255	0	220	255	140	0
26	0	103	255	91	0	255	145	156	114	255	0	221	255	135	0
27	0	107	255	92	0	255	142	157	118	255	0	222	255	132	0
28	0	111	255	93	0	255	137	158	122	255	0	223	255	127	0
29	0	115	255	94	0	255	134	159	126	255	0	224	255	123	0
30	0	119	255	95	0	255	129	160	129	255	0	225	255	119	0
31	0	123	255	96	0	255	126	161	134	255	0	226	255	115	0
32	0	127	255	97	0	255	122	162	137	255	0	227	255	111	0
33	0	132	255	98	0	255	118	163	142	255	0	228	255	107	0
34	0	135	255	99	0	255	114	164	145	255	0	229	255	103	0
35	0	140	255	100	0	255	110	165	150	255	0	230	255	99	0
36	0	143	255	101	0	255	106	166	153	255	0	231	255	95	0
37	0	148	255	102	0	255	102	167	158	255	0	232	255	91	0
38	0	151	255	103	0	255	98	168	161	255	0	233	255	87	0
39	0	156	255	104	0	255	94	169	166	255	0	234	255	83	0
40	0	159	255	105	0	255	90	170	169	255	0	235	255	79	0
41	0	164	255	106	0	255	86	171	174	255	0	236	255	75	0
42	0	167	255	107	0	255	82	172	177	255	0	237	255	71	0
43	0	172	255	108	0	255	78	173	182	255	0	238	255	67	0
44	0	175	255	109	0	255	74	174	185	255	0	239	255	63	0
45	0	180	255	110	0	255	70	175	190	255	0	240	255	59	0
46	0	183	255	111	0	255	66	176	193	255	0	241	255	55	0
47	0	188	255	112	0	255	61	177	198	255	0	242	255	51	0
48	0	191	255	113	0	255	57	178	201	255	0	243	255	47	0
49	0	196	255	114	0	255	53	179	206	255	0	244	255	43	0
50	0	199	255	115	0	255	49	180	209	255	0	245	255	39	0
51	0	204	255	116	0	255	45	181	214	255	0	246	255	35	0
52	0	207	255	117	0	255	41	182	217	255	0	247	255	31	0

Table 2   (*Continued*)

ID	R	G	B	ID	R	G	B	ID	R	G	B	ID	R	G	B
53	0	212	255	**118**	0	255	37	**183**	222	255	0	**248**	255	27	0
54	0	215	255	**119**	0	255	33	**184**	225	255	0	**249**	255	23	0
55	0	220	255	**120**	0	255	29	**185**	230	255	0	**250**	255	19	0
56	0	223	255	**121**	0	255	25	**186**	233	255	0	**251**	255	15	0
57	0	228	255	**122**	0	255	21	**187**	238	255	0	**252**	255	11	0
58	0	231	255	**123**	0	255	17	**188**	241	255	0	**253**	255	7	0
59	0	236	255	**124**	0	255	13	**189**	246	255	0	**254**	255	3	0
60	0	239	255	**125**	0	255	9	**190**	249	255	0	**255**	255	0	0
61	0	244	255	**126**	0	255	5	**191**	254	255	0				
62	0	247	255	**127**	0	255	1	**192**	255	252	0				
63	0	252	255	**128**	1	255	0	**193**	255	247	0				
64	0	255	254	**129**	5	255	0	**194**	255	244	0				

Other color scales with various combination of *red*, *green*, and *blue* color components are also possible [19], and users can design their own color scale which is more suitable to fulfill their needs. Principally, one thing that should be considered in data presentation is that the purpose of coloring the radiometric raw data is to make the interpretation of the data in a more effective and efficient way and an accurate decision can be achieved.

5.0   CONCLUSION

This paper demonstrates the use of numerical heat conduction modelling to simulate the real situation of thermal properties of object of interest. This data is then used to generate the synthetic thermal image. The way of visualization that has been described in the text is both for the generation of a grayscale and color thermogram. Synthetic thermogram gives many advantages to thermographers, since they can simulate the real situation without any need to fabricate the specimen and they can test their developed image processing algorithms in case the real thermograms are difficult to obtain.

REFERENCES

[1]   Kaplan, H. 1993. *Practical Applications of Infrared Thermal Sensing and Imaging Equipment*. Washington: SPIE-The International Society for Optical Engineering.

[2]   Maldague, X. P. V. (ed.). 1994. *Infrared Methodology and Technology*. Amsterdam: Gordon and Breach Science Publishers S. A.

[3]   Levitt, J. 2003. *Complete Guide to Preventive and Predictive Maintenance*. New York: Industrial Press, Inc.

[4]   Maldague, X. P. V. 2001. *Theory and Practice of Infrared Technology for Nondestructive Testing*. New York: John Wiley & Sons, Inc.

[5]   Nowakowski, A., M. Kaczmarek and J. Rumiñski. 2002. Synthetic Pictures in Thermographic Diagnostics. *Proceedings of the Second Joint EMBS/BMES Conference, Houston, USA, October 23-26, 2002*. 1131-1132.

[6]   Weijie, Y., T. Hongming and P. Qunsheng. 1998. An Infrared Image Synthesis Model based on Infrared Physics and Heat Transfer. *International Journal of Infrared and Millimeter Waves*. 19(12): 1661-1669.

[7]   Gambotto, J. P. 1994. Combining Image Analysis and Thermal Models for Infrared Scene Simulations. *Proceedings of IEEE International Conference on Image Processing 1994 (ICIP '94), Austin, Texas, USA, November 13-16, 1994.* 710-714.

[8]   Evans, R. J. 1991. Simulation in Infrared Imaging: using Electrical Circuit Principles to Model Heat Transfer. *Proceedings of the IEEE National Aerospace and Electronics Conference, Dayton, OH, May 20-24, 1991.* 2: 907-913.

[9]   Oh, C., N. Nandhakumar and J. K. Aggarwal. 1989. Integrated Modelling of Thermal and Visual Image Generation. *Proceedings of IEEE Computer Society Conference on Computer Vision and Pattern Recognition (CVPR '89), San Diego, CA, USA, June 4-8, 1989.* 356-362.

[10]   ElShayeb, M. and Y. K. Beng. 2000. *Application of Finite Difference and Finite Element Methods for Thermal Problems.* Sabah: Universiti Malaysia Sabah.

[11]   Cone, C. 1980. *Energy Management for Industrial Furnaces.* New York: John Wiley & Sons, Inc.

[12]   Griswold, J. 1946. *Fuels, Combustion, and Furnaces.* McGraw-Hill Book Company, Inc.

[13]   Planchard, D. C. and M. P. Planchard. 2005. *Engineering Design with Solid Works 2005: A Step-by-step Project Based Approach Utilizing 3D Solid Modeling.* SDC Publications.

[14]   Structural Research and Analysis Corporation. 2003. *Introducing COSMOS Works.* Los Angeles, California: SRAC.

[15]   Aliev, R. A. and R. R. Aliev. 2001. *Soft Computing and Its Applications.* Singapore: Word Scientific Publishing Company.

[16]   Gonzalez, R. C., R. E. Woods, and S. L. Eddins. 2004. *Digital Image Processing using MATLAB.* Upper Saddle River, NJ: Pearson Eduction, Inc.

[17]   Jähne, B. 2005. *Digital Image Processing.* 6th revised and extended edition. Springer-Verlag Berlin Heidelberg.

[18]   Gonzalez, R. C. and R. E. Woods. 2002. *Digital Image Processing.* 2nd Edition. Upper Saddle River, NJ: Prentice-Hall, Inc.

[19]   Levkowitz, H. and G. T. Herman. 1992. Color Scales for Image Data. *IEEE Computer Graphics & Applications.* 72-80.

[20]   Bourke, P. Colour Ramping for Data Visualization. http://local.wasp.uwa.edu.au/~pbourke/texture_colour/ colorramp/ (Accessed on June 4, 2007).

[21]   Crane, R. 1997. *A Simplified Approach to Image Processing: Classical and Modern Techniques in C.* Upper Saddle River, NJ: Prentice Hall PTR.

[22]   Munir, R. 2004. *Pengolahan Citra Digital dengan Pendekatan Algoritmik.* Bandung, Indonesia: Penerbit Informatika.

[23]   Trinks, W., M. H. Mahinney, R. A. Shannon, R. J. Reed, and J. R. Garvey. 2004. *Industrial Furnaces.* 6th ed. John Wiley & Sons, Inc.